



X International Conference on Structural Dynamics, EURODYN 2017

Analytical, numerical and experimental studies on the Semi-Active Friction Tendon

Hernán Garrido^{a*}, Oscar Curadelli^a, Daniel Ambrosini^a

^a CONICET, National University of Cuyo, Eng. Faculty, Mendoza (5502), Argentina

Abstract

For controlling vibrations, a Semi-Active Friction Tendon (SAFT), which consists of a semi-active friction damper and an auxiliary spring that are linked to the structure by a cable, is studied experimentally, numerically and analytically. Two semi-active control laws are implemented, one is based on velocity feedback (denoted as SQDCL) and the other is based on force feedback (denoted as SPCL); the passive control case is also studied for comparison. Based on the structural displacement reduction and the hysteretic behavior assessment, it is clearly demonstrated that (for SAFTs with a given pre-tension force): (1) the effectiveness of the optimized passive-control case can always be improved by using semi-active control with any of the two control laws; and (2) the SPCL is more effective for large displacements, while the SQDCL is more advantageous for very small displacements. Moreover, closed-form expressions for the dissipated energy are presented for the three cases under consideration, which can be used in preliminary design of SAFTs to decide between passive and semi-active control and to choose the more suitable control law.

© 2017 The Authors. Published by Elsevier Ltd.

Peer-review under responsibility of the organizing committee of EURODYN 2017.

Keywords: vibration control; semi-active control; friction; cable slackening; hysteretic behavior

1. Introduction

Vibrations can be problematic in different types of structures (either civil, mechanical, aerospace, industrial, home appliances, etc.); namely, they can cause discomfort in people due to floor vibration or ambient noise, malfunctioning of sensitive instruments, and structural deterioration. To mitigate these problems, many methodologies have been proposed and implemented in real cases [1,2]. These can be classified into: (1) passive

* Corresponding author. Tel.: +54-261-4135000 Int. 2195.

E-mail address: carloshernangarrido@gmail.com

control (PC), which uses constant-parameters devices to dissipate energy; (2) active control (AC), which uses actuators capable of exerting forces arbitrarily on the structure; and (3) semi-active control (SAC), which uses devices whose parameters are smartly adjusted in real-time. SAC is attractive because, in general, it is more effective and robust against parameter variation than PC and it requires much less power to operate than AC [3].

Regardless of the type of control, the mechanical connection of control devices to the vibrating structure is of extreme importance because of its influence in the control effectiveness. In particular, because of architectural restrictions, or if the structure is very slender or has variable geometry (as deployable space structures [4]), the use of traditional braces can become impractical. An appropriate mechanical arrangement that includes pre-tensioned cables is a possible alternative solution.

In the context of SAC applied to cable-linked dampers, Klein and Healey [5] proposed the coupling of two buildings with cables that could be released and tightened to provide specified dissipative control forces. Erramouspe et al. [6] studied a semi-active damper using two pre-tensioned cables, in order to implement a resetting stiffness controller. In a recent work [7], it was proposed a device named Semi-Active Friction Tendon (SAFT) for the vibration control of space structures (requiring only one cable per damper) which consists of a friction damper in parallel with a soft auxiliary spring, both linked to the structure by means of a cable.

The present paper studies numerically and experimentally the effectiveness of SAFTs with PC and SAC, under a control law based on velocity-feedback denoted as Simplified Quickest Descent Control Law (SQDCL) and a control law based on force-feedback, denoted as Slackening Preventing Control Law (SPCL). Hysteretic behavior of SAFTs is analytically studied and compared to experimental and numerical results. Closed-form expressions for the energy dissipated per cycle are obtained as functions of the system parameters and the maximum displacement. The results derived in the present paper allow estimating expectable performance in different application cases, e.g. civil and mechanical structures.

2. Vibration control system based on SAFTs

Fig. 1 schematically shows two SAFTs connected in opposition to a single-degree-of-freedom (SDOF) structure, indicating: displacement, mass, stiffness, and damping coefficient of the structure as q_s , m_s , k_s and c_s , respectively; displacement, mass, friction coefficient, and normal force of the i -th friction damper as q_{di} , m_{di} , μ_i , and N_i , respectively; pre-tension displacement and stiffness of the i -th auxiliary spring as Δ_{0i} and k_{di} , respectively; and tensile stiffness of the i -th cable as k_{ci} . The constant parameter L_i is the final length of the i -th SAFT in static pre-tensioned state; whereas L_{0ci} and L_{0di} are the natural lengths (without pre-tension) of the cable and auxiliary spring, respectively, of the i -th SAFT.

The SAFTs can operate with PC, where N_i is constant during the operation; or SAC, where N_i is continuously adjusted during the operation by one predefined control law (SQDCL or SPCL). SQDCL reduces N_i when structure approaches the SAFT whereas SPCL reduces N_i when cable force is under a small threshold v_F .

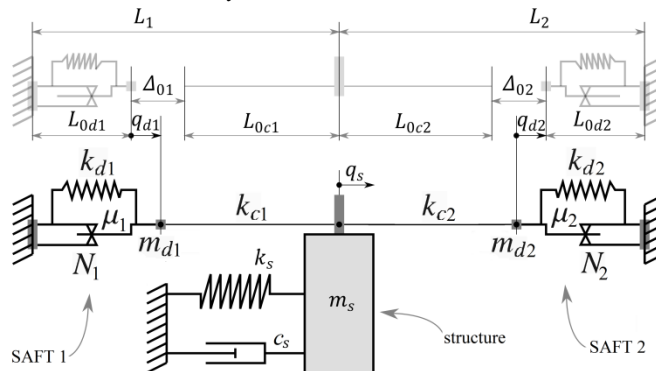


Fig. 1. Two SAFTs connected to a SDOF structure; grey lines indicate undeformed shape and black lines indicate pre-tensioned shape.

The equations of motion for the system shown in Fig. 1 can be found in [7]. Concisely, the dynamic model has 3 degrees-of-freedom and the only non-linearities considered are Coulomb friction at the dampers and slackening at the cables.

3. Hysteretic behavior of a SAFT

The usability of any damping-based vibration control method strongly depends on the specific application case, i.e.: required damping/energy dissipation, stringency of vibration limits, geometrical and physical constraints, technological aspects. In this context, the hysteretic behavior of dissipative devices could be used in first instance to compare different control alternatives.

In this section, analytical constructions of hysteresis loops (i.e. the relations between structure displacement q_s and cable force F_c) are made neglecting the external- and inertial-forces on friction dampers. It is assumed that the structure imposes a cyclic displacement with constant amplitude on the SAFT.

Fig. 2(a) shows the hysteresis loop of SAFT using PC. Its main characteristics are: (1) the forward-friction branch (3-4) is symmetric to the backward-friction branch (6-1), being both equally dependent on N ; and (2) both, the loading and unloading branches (1-3 and 4-6), have a slope approximately equal to the cable stiffness k_c ($k_c \gg k_d$).

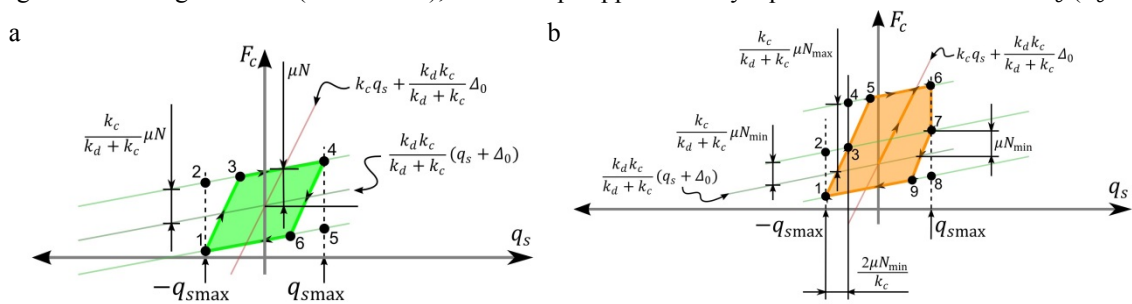


Fig. 2. Analytical construction of hysteresis loop with: (a) PC; (b) SAC under SQDCL.

From geometrical considerations, the following general expression can be found to approximate the energy dissipated per cycle when using PC [8]:

$$E_{D(PC)} \approx \begin{cases} 4q_{smax}\mu N & \text{if } \mu N < k_d(\Delta_0 - q_{smax}) \\ 2\mu N q_{smax} + 2\mu N \Delta_0 - \frac{2(\mu N)^2}{k_d} & \text{if } k_d(\Delta_0 - q_{smax}) \leq \mu N < k_d \Delta_0 \\ 0 & \text{if } q_{smax} \leq \frac{\mu N}{k_c} \end{cases} \quad (1)$$

Hysteresis loop shown in Fig. 2(b) can be constructed for SAC with the SQDCL. Two aspects are worth mentioning: (1) the enclosed area can be increased upward by increasing N_{max} , without modifying the backward-friction branch (9-1) (which could induce cable slackening); and (2) the unloading branch (6-7-9) has an abrupt drop (6-7) showing a phenomenon sometimes called resetting stiffness [9], which stands out for displaying energy dissipation without friction. As with PC, the following expression is obtained to approximate the energy dissipated per cycle when SQDCL is used:

$$E_{D(SQDCL)} \approx \begin{cases} 2q_{smax}(\mu N_{max} + \mu N_{min}) & \text{if } \mu N_{min} < k_d(\Delta_0 - q_{smax}) \\ 0 & \text{if } q_{smax} \leq \frac{\mu N_{min}}{k_c} \end{cases} \quad (2)$$

When comparing Eqs. (1) and (2) for $N = N_{max}$ and the same pre-tension Δ_0 , it is observed that $E_{D(SQDCL)} < E_{D(PC)}$ if cables are taut. However, N_{max} can be designed much larger than N , still avoiding cable slackening, in such a way that $E_{D(SQDCL)} \gg E_{D(PC)}$. For this reason, SAC under the SQDCL is expected to make SAFTs more effective than with PC. Moreover, the vibration level below which the SAFT is ineffective (stringency) depends on N for PC, but on N_{min} for SAC. Thus, SAC gives effectiveness independency between large and small vibrations.

Finally, hysteresis loops of SAC with the SPCL are addressed for large- and very-small-displacements separately, as shown in Fig. 3. Particularly in Fig. 3(d), it is evident that SPCL does not exhibit resetting stiffness phenomenon.

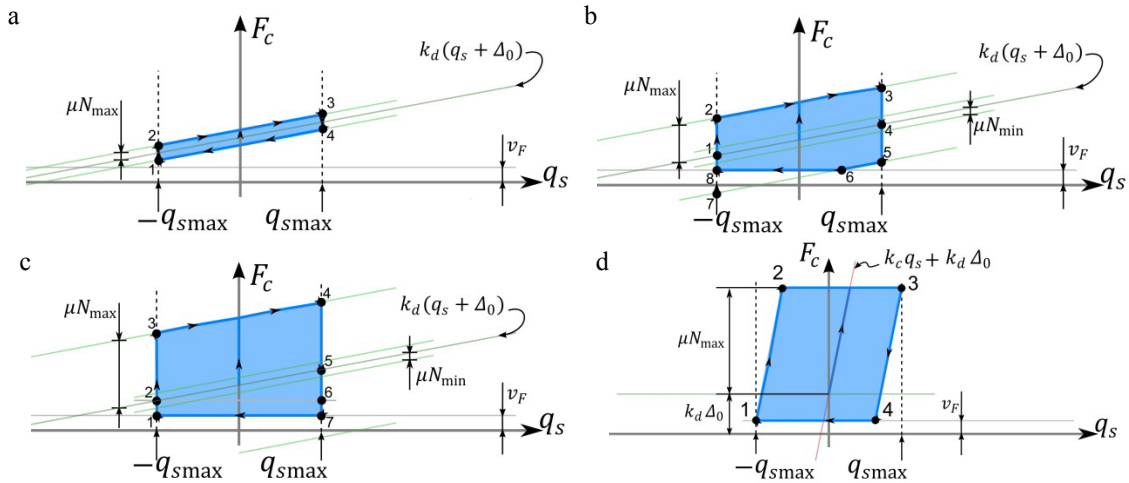


Fig. 3. Analytical construction of hysteresis loops with SAC under SPCL for: (a-c) large displacements; (d) very-small displacements.

Analogously to the previous cases, the energy dissipated per cycle is approximated for the four characteristic cases of Fig. 3 as follows:

$$E_{D(SPCL)} \approx \begin{cases} 4\mu N_{\max} q_{s\max} & \text{if } \mu N_{\max} \leq k_d(\Delta_0 - q_{s\max}) - v_F, \\ 2q_{s\max}(\mu N_{\max} + k_d\Delta_0 - v_F) & \text{if } \mu N_{\max} \geq k_d(\Delta_0 + q_{s\max}) - v_F, \\ 4\mu N_{\max} q_{s\max} - \frac{(\mu N_{\max} - k_d(\Delta_0 - q_{s\max}) + v_F)^2}{2k_d} & \text{if } k_d(\Delta_0 - q_{s\max}) - v_F \leq \mu N_{\max} \leq k_d(\Delta_0 + q_{s\max}) - v_F \\ 0 & \text{if } q_{s\max} \lesssim \frac{\mu N_{\max} + k_d\Delta_0 - v_F}{2k_c} \end{cases} \quad (3)$$

It can be seen that, as with SQDCL, dissipated energy can be increased through N_{\max} avoiding risk of cable slackening in the backward-friction branch. However, $E_{D(SQDCL)} < E_{D(SPCL)}$, making SPCL the most suited for large displacements, i.e. when $q_{s\max} \gg \mu N_{\max}/k_c$. On the other hand, for very-small displacements, SPCL is less suitable since the vibration level below which the SAFT is ineffective depends on N_{\max} , i.e. the same parameter that sets the large-displacement effectiveness.

Another important aspect to highlight is the sensitivity of (optimal) dissipated energy to loss of pre-tension. While, in PC, optimal $E_{D(PC)}$ is strongly dependent on Δ_0 (second row of Eq. (1)); in SAC, optimal $E_{D(SQDCL)}$ is independent on Δ_0 (first row of Eq. (2)) and optimal $E_{D(SPCL)}$ is relatively dependent on Δ_0 (second row of Eq. (3)). Note that, in PC, Δ_0 must be designed similar to $q_{s\max}$ (or, preferably, much larger) to avoid cable slackening while, in SAC, Δ_0 can be designed such that $\mu N_{\max} \gg k_d\Delta_0$.

4. Numerical and experimental results

In order to assess the performance of a structure controlled by two SAFTs with PC and SAC, shaking table tests were carried out by using the experimental setup shown in Fig. 4(a) and schematized in Fig. 4(b). The acceleration record consisted in a frequency sweep from 1/5 to 5 times the fundamental frequency of the structure.

Numerical simulations based on the mathematical model of section 2 were carried out in MATLAB/Simulink using a stiff fifth-order implicit integration method with variable time step (ode15s).

Fig. 5 shows characteristic hysteresis loops that were recorded during tests along with the corresponding numerical simulations. For PC, Fig. 5(a) resembles the classical bilinear hysteretic model, because the cable is taut.

For SQDCL, Fig. 5(b) shows instantaneous cable forces are not accurately predicted by the numerical model however the enclosed area and peak forces fit acceptably (which are important for performance prediction and cable design). Finally, the contrast between Fig. 5(b) and (c) evidences the resetting stiffness phenomenon, which is present in SQDCL and absent in SPCL. It is also noted that the analytically constructed shapes shown in Fig. 2 and Fig. 3 are good approximations of those shown in Fig. 5.

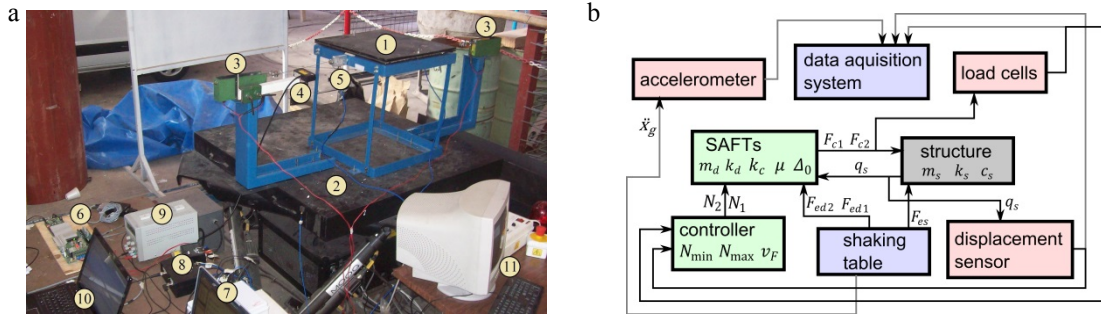


Fig. 4. Experimental setup. (a) general view: (1) structure, (2) shaking table, (3) SAFTs, (4) displacement sensor, (5) load cell, (6) controller, (7) data acquisition system, (8) signal conditioners, (9) power supply, (10) and (11) personal computers; (b) simplified block diagram.

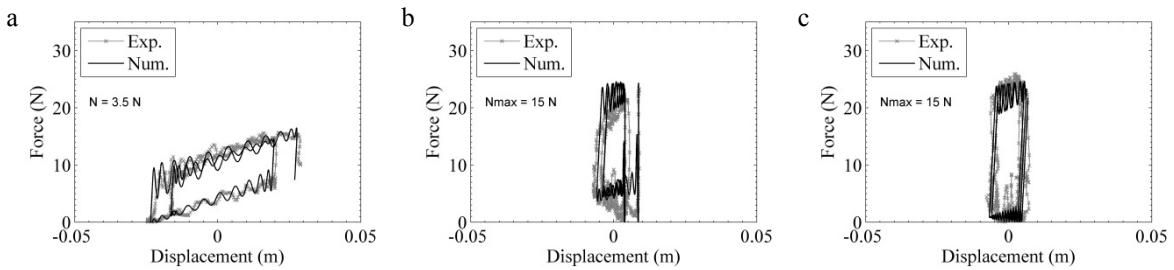


Fig. 5. Hysteresis loops with: (a) PC; (b) SAC under SQDCL; (c) SAC under SPCL.

Fig. 6(a) shows an effectiveness index based on RMS displacement reduction for the three studied cases (numerically and experimentally). As can be seen, displacements are drastically reduced as compared to the uncontrolled case (i.e., $J_{rms} = 1$). Moreover, numerical simulations accurately estimate the experimentally-obtained effectiveness index. Fig. 6(b) is a plot of Eqs. (1-3); when comparing it to Fig. 6(a), it is clear the relationship between analytically-predicted dissipated energy and observed performance. That is, PC exhibits an optimal normal force whereas SAC can always be improved by enlarging the maximum normal force. Besides SPCL, which dissipates more energy per cycle (Fig. 6(b)), also displays more effectiveness (Fig. 6(a)).

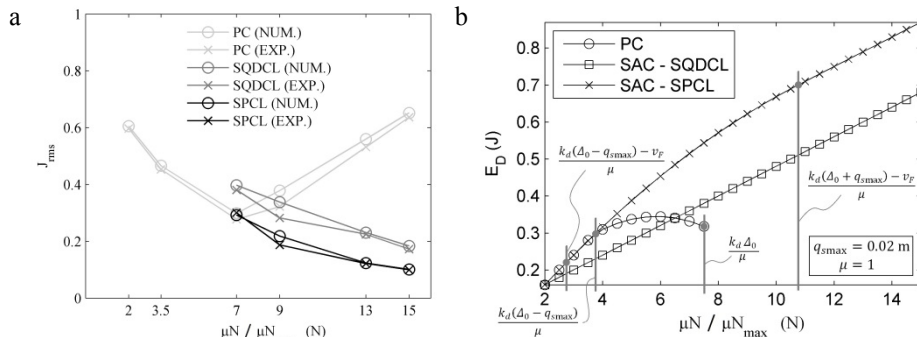


Fig. 6. (a) Effectiveness of the control system in terms RMS displacement reduction; (b) energy dissipated per cycle, for large displacements.

5. Conclusions

In this paper, shaking table tests, numerical simulations, and analytical developments were briefly shown to compare the effectiveness of SAFTs under PC and SAC with two different control laws (SQDCL and SPCL).

The main conclusions of the present work are:

(1) A simple lumped-nonlinearities model is accurate enough for: (1) assessing the effectiveness in displacement reduction and (2) sizing the cables, anchorages and dampers.

(2) For a given pre-tension force, the achievable effectiveness with SAC is always superior to that with PC, irrespective of the chosen control law.

(3) If structure displacements are much larger than cable stretching (i.e., effect of cable stiffness is negligible), the achievable effectiveness with SPCL is superior to that with SQDCL.

(4) If the structure displacements are comparable to cable stretching (i.e., effect of cable stiffness is not negligible), the SPCL can become ineffective while the SQDCL is still effective (in terms of energy dissipation).

(5) Regarding robustness to loss of pre-tension, SAC provides lower sensitivity than PC, especially when SQDCL is used.

These conclusions suggest that the SQDCL is more appropriate for applications involving stringent vibration limits, e.g. large space structures or precision equipment; whereas the SPCL is more appropriate where strong displacement reduction is needed only during large loads, e.g. vibration control of civil structures under seismic events. Last but not least, SAC should be considered only if PC does not achieve the application requirements.

Notwithstanding these suggestions, it is remarked that the closed-form expressions derived in this paper for the “energy dissipated per cycle” can be used as an engineering tool in the preliminary design SAFTs. This includes the comparison with other alternatives, the non-trivial decision to use PC or SAC and the choice of the control law. Moreover, these closed-form expressions can be used in linearization techniques for fast response analysis.

Acknowledgements

The authors would like to thank National Research Council from Argentina (CONICET) and National University of Cuyo for the financial support.

References

- [1] T.T. Soong, G.F. Dargush, *Passive Energy Dissipation Systems in Structural Engineering*, John Wiley & Sons, Chichester, UK, 1997.
- [2] F. Casciati, J. Rodellar, U. Yildirim, Active and semi-active control of structures - theory and applications: A review of recent advances, *J. Intell. Mater. Syst. Struct.* 23 (2012) 1181-1195. doi:10.1177/1045389X12445029.
- [3] F. Casciati, G. Magonette, F. Marazzi, *Technology of Semiactive Devices and Applications in Vibration Mitigation*, John Wiley & Sons, Ltd, Chichester, UK, 2006. doi:10.1002/0470022914.
- [4] G. Tibert, *Deployable Tensegrity Structures for Space Applications*, Royal Institute of Technology, 2002.
- [5] R.E. Klein, M.D. Healey, Semi-active control of wind induced oscillations in structures, en: H.H.E. Leipholz (Ed.), *Second Int. Symp. Struct. Control*, Martinus Nijhoff Publishers, Ontario, Canada, 1985: pp. 354-369.
- [6] J. Erramouspe, P. Kioussis, R. Christenson, T. Vincent, A resetting stiffness dynamic controller and its bench-scale implementation, *Eng. Struct.* 29 (2007) 2602-2610. doi:10.1016/j.engstruct.2007.01.014.
- [7] H. Garrido, O. Curadelli, D. Ambrosini, Semi-active friction tendons for vibration control of space structures, *J. Sound Vib.* 333 (2014) 5657-5679. doi:10.1016/j.jsv.2014.06.018.
- [8] H. Garrido, O. Curadelli, D. Ambrosini, Experimental and theoretical study of semi-active friction tendons, *Mechatronics.* 39 (2016) 63-76. doi:10.1016/j.mechatronics.2016.08.005.
- [9] L.-Y. Lu, G.-L. Lin, Improvement of near-fault seismic isolation using a resettable variable stiffness damper, *Eng. Struct.* 31 (2009) 2097-2114. doi:10.1016/j.engstruct.2009.03.011.